SLAC-PUB-95-7052
November, 1995

Measurement of Subpicosecond Electron Bunch Lengths*

Hung-chi Lihn†, David Bocek‡, Pamela Kung, Chitrlada Settakorn, and Helmut Wiedemann

Applied Physics Department, ‡Physics Department, and Stanford Linear Accelerator Center, Stanford University, Stanford, California 94309

Abstract. A new frequency-resolved bunch-length measuring system has been developed at the Stanford SUNSHINE facility suitable for subpicosecond electron bunches. This method utilizes a far-infrared Michelson interferometer to measure coherent transition radiation emitted from electron bunches through optical autocorrelation. A simple and systematic way has also been developed to include interference effects caused by the beam splitter, so the electron bunch length can be easily obtained from the measurement. This autocorrelation method demonstrates subpicosecond resolving power that cannot be achieved by existing time-resolved methods.

INTRODUCTION

In recent years, the production of short electron bunches, especially in the subpicosecond regime, has become an interesting aspect in the development of particle accelerators. It greatly affects the design of next-generation synchrotron light sources, future linear colliders, free-electron lasers, and high-intensity coherent far-infrared light sources. Hence, a bunch-length measuring system capable of characterizing subpicosecond pulses will provide a powerful tool for this development.

As a direct approach, a time-resolved method resolves a beam-generated signal in the time domain to measure the bunch distribution. However, existing fast time-resolved methods such as the streak camera do not provide enough

*Work supported by Department of Energy contract DE–AC03–76SF00515.

†E-mail: Lihn@Slac.Stanford.edu

Presented at Micro Bunches: The Workshop on The Production Measurements and Applications of Short Bunches of Electrons and Positions in Linacs and Storage Rings, Upton, L.I., New York, September 28–30, 1995.

resolving power for bunch lengths in the subpicosecond regime; nevertheless, the hardware has already become very complicated and expensive. On the other hand, a frequency-resolved technique extracts the frequency content of a beam-generated signal. From this frequency information, the particle distribution can be deduced. Unlike the time-resolved technique, it does not require fast processing speed and complex hardware. Since the necessary broad bandwidth required for short pulses can be achieved by optical methods, a good subpicosecond time resolution can be easily obtained. This is a well-known technique used in the characterization of femtosecond laser pulses(1) and has been suggested for subpicosecond bunch-length measurements(2).

At the SUNSHINE facility, we have developed a new bunch-length measuring system based on this frequency-resolved technique. Using subpicosecond electron pulses generated at SUNSHINE(3,4), we have demonstrated that it is a simple and low-cost instrument suitable for subpicosecond bunch-length measurements(5). In this paper, we will describe the principle of this autocorrelation technique, analysis and interpretation of bunch-length measurements, and experimental results.

AUTOCORRELATION BUNCH-LENGTH MEASURING METHOD

As a frequency-resolved method, this method uses a far-infrared Michelson interferometer to measure the spectrum of coherent transition radiation via optical autocorrelation. Coherent transition radiation emitted by electron pulses carries the information of bunch distribution in its frequency content. By analyzing the frequency information, the bunch length can be derived.

Coherent Transition Radiation

Transition radiation is generated when an electron passes the interface of two media of different dielectric constants(6). For a vacuum-metal interface, the spectrum of transition radiation is approximately constant in the far-infrared regime due to the almost perfect conductivity of the metal. The radiated intensity from a relativistic electron has a zero at $\theta = 0$ and reaches maximum at $\theta \sim 1/\gamma$, where θ is the angle between the radiation and the electron direction, and γ is the Lorentz factor.

When a bunch of N electrons passes the interface, the resulting total intensity at wavelength λ can be expressed as(7)

$$I_{\text{total}}(\lambda) = N[1 + (N-1)f(\lambda)]I_e(\lambda), \tag{1}$$

where $I_e(\lambda)$ is the intensity of transition radiation emitted by an electron at wavelength λ. In the far-infrared regime, $I_e(\lambda)$ is constant. The form factor

$f(\lambda)$ is given by the three-dimensional Fourier transform of the normalized bunch distribution $W(\mathbf{r})$, where $\int W(\mathbf{r})d\mathbf{r} = 1$,

$$f(\lambda) = \left| \int W(\mathbf{r}) e^{i2\pi(\hat{\mathbf{n}}\cdot\mathbf{r})/\lambda} d\mathbf{r} \right|^2, \qquad (2)$$

where $\hat{\mathbf{n}}$ is the unit vector directed from the center of the bunch to the observation point and $\mathbf{r}$ the position vector of an electron relative to its bunch center. If the radiation is observed in the forward direction (which is defined as the unit vector $\hat{\mathbf{z}}$ and $\hat{\mathbf{n}} \parallel \hat{\mathbf{z}}$) from a transversely symmetric beam, the form factor $f(\lambda)$ is only determined by the longitudinal bunch distribution.

However, transition radiation does not produce radiation in the forward direction $[\theta = \cos^{-1}(\hat{\mathbf{n}} \cdot \hat{\mathbf{z}}) = 0]$. In order to use transition radiation to measure the bunch length, observing the radiation in an off-axis direction ($\theta \neq 0$) is necessary. In this case, the transverse bunch distribution will contribute to the form factor even for a transversely symmetric beam. Minimizing such contribution becomes important for clean subpicosecond bunch-length measurements. For example, the form factor for a cylindrical beam of radius ρ and length l, when observed at an angle θ, is given by

$$f(\lambda)\Big|_\theta = 4\left[\frac{J_1(2\pi\rho\sin\theta/\lambda)}{2\pi\rho\sin\theta/\lambda}\frac{\sin(\pi l\cos\theta/\lambda)}{\pi l\cos\theta/\lambda}\right]^2, \qquad (3)$$

where J_1 is the first order Bessel function. In the forward direction ($\theta = 0$), the transverse contribution vanished. However, for large angles or big transverse beam sizes, the transverse contribution will result in an apparent bunch-length measurement that is longer than the actual one. This transverse contribution, however, can be ignored if the condition $2\pi\rho\tan\theta/3.83 \ll l$ is satisfied, which is assumed through out this paper. Hence, good focusing to produce small transverse beam size and a reasonable angular acceptance for the detector is crucial for accurate subpicosecond bunch-length measurements.

Michelson Interferometer

Since the spectrum of coherent transition radiation emitted by subpicosecond electron bunches is in the far-infrared regime, a far-infrared Michelson interferometer is used to measure the spectrum via optical autocorrelation. The interferometer is shown schematically in Fig. 1. It consists of a beam splitter, a fixed and a movable mirror, and a detector. When light enters the Michelson interferometer, the beam splitter splits its amplitude into two mirror arms. As these two rays are reflected from the mirrors, they are recombined at the beam splitter and sent into the detector.

An ideal beam splitter has constant amplitude reflection (R) and transmission (T) coefficients over all frequencies, which satisfy $|R|^2 = |T|^2 = 1/2$.

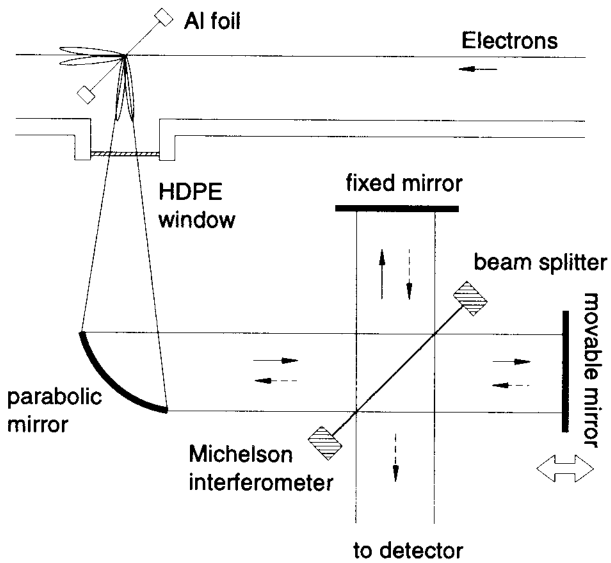

FIGURE 1. Schematic diagram of a Michelson interferometer for bunch-length measurements.

As shown in Fig. 1, for an incoming light pulse of electric field E with intensity proportional to $|E|^2$, the light pulse split by the beam splitter and reflected by the fixed mirror has a field amplitude of TRE when it reaches the detector; on the other hand, the light pulse reflected by the movable mirror has an amplitude of RTE at the detector. Note that perfect reflection on the mirrors is assumed. At zero optical path difference, the pulses completely overlap at the detector, and the total intensity reaches the maximum $|2RTE|^2 = 4|RT|^2|E|^2 = |E|^2$. As the path difference increases but is still shorter than the bunch length, the two pulses overlap partially, and the total intensity decreases. When the path difference of two arms is larger than the bunch length, the two pulses are totally separated in time, and the resulting intensity at the detector is $2|RT|^2|E|^2 = |E|^2/2$. The intensity is constant over all path differences greater than the bunch length and is called the *baseline.* The variation of intensity about the baseline as a function of optical path difference is defined as the *interferogram.* Therefore, the width of the peak in the interferogram can be used to estimate the bunch length. For example, the bunch length is equal to the full width at half maximum (FWHM) of the interferogram for a rectangular bunch distribution; however, for a Gaussian bunch distribution, its equivalent bunch length ($\sqrt{2\pi}\,\sigma_z$) is about 75% of the interferogram FWHM.

The intensity of the recombined radiation at the detector can be expressed in the time domain with an additional time delay δ/c for the movable arm by

$$I(\delta) \;\propto\; \int_{-\infty}^{+\infty} \left|TRE(t) + RTE(t+\frac{\delta}{c})\right|^2 \mathrm{d}t$$

$$= 2|RT|^2 \,\mathrm{Re}\int_{-\infty}^{+\infty} E(t)E^*(t+\frac{\delta}{c})\mathrm{d}t + 2|RT|^2 \int_{-\infty}^{+\infty} |E(t)|^2 \,\mathrm{d}t, \quad (4)$$

or in the frequency domain with a phase factor $e^{-i\omega\delta/c}$ for the movable arm by

$$\begin{aligned} I(\delta) &\propto \int_{-\infty}^{+\infty} \left|TR\tilde{E}(\omega) + RT\tilde{E}(\omega)e^{-i\omega\delta/c}\right|^2 \mathrm{d}\omega \\ &= 2\,\mathrm{Re}\int_{-\infty}^{+\infty} |RT|^2|\tilde{E}(\omega)|^2 e^{-i\omega\delta/c}\mathrm{d}\omega + 2\int_{-\infty}^{+\infty} |RT|^2|\tilde{E}(\omega)|^2\mathrm{d}\omega, \quad (5) \end{aligned}$$

where δ is the optical path difference and c the speed of light. Equations (4) and (5) are related by the Fourier transform $\tilde{E}(\omega) = \frac{1}{\sqrt{2\pi}}\int_{-\infty}^{+\infty} E(t)e^{i\omega t}\mathrm{d}t$. The baseline is defined as the intensity at $\delta \to \pm\infty$, i.e.,

$$I_\infty \propto \begin{cases} 2|RT|^2 \int_{-\infty}^{+\infty} |E(t)|^2\mathrm{d}t & \text{(time domain)}, \\ 2\int_{-\infty}^{+\infty} |RT|^2|\tilde{E}(\omega)|^2\mathrm{d}\omega & \text{(frequency domain)}. \end{cases} \quad (6)$$

By definition, the interferogram can be written as

$$\begin{aligned} S(\delta) &= I(\delta) - I_\infty \\ &\propto \begin{cases} 2|RT|^2\,\mathrm{Re}\int_{-\infty}^{+\infty} E(t)E^*(t+\frac{\delta}{c})\mathrm{d}t & \text{(time domain)}, \\ 2\,\mathrm{Re}\int_{-\infty}^{+\infty} |RT|^2|\tilde{E}(\omega)|^2 e^{-i\omega\delta/c}\mathrm{d}\omega & \text{(frequency domain)}. \end{cases} \end{aligned} \quad (7)$$

Therefore, the interferogram $S(\delta)$ is the autocorrelation of the incident light pulse, and its Fourier transform is the power spectrum of the pulse. Solving for $|\tilde{E}(\omega)|^2$ in Eq. (7) and using Eq. (1) with the relation $I_{\mathrm{total}}(\lambda) \propto |\tilde{E}(2\pi c/\lambda))|^2$, the bunch form factor can be obtained by

$$f(\lambda) \propto \frac{1}{N-1}\left[\frac{1}{4\pi c|RT|^2 N I_e(\lambda)}\int_{-\infty}^{+\infty} S(\delta)e^{i2\pi\delta/\lambda}\mathrm{d}\delta - 1\right], \quad (8)$$

where $|\tilde{E}(\omega)|^2 = |\tilde{E}(-\omega)|^2$ is used since $E(t)$ is a real function. Hence, the interferogram contains the frequency spectrum of coherent transition radiation and can be used to derive the bunch length.

Beam-Splitter Interference Effects

Suitable beam splitters for the far-infrared regime (a Mylar foil in our design) do not provide constant and equal reflectance and transmittance for all frequencies. This is caused by the interference of light reflected from both surfaces of the beam splitter, which is equivalent to thin-film interference in optics(8). The total amplitude reflection and transmission coefficients for a Mylar foil of thickness t and refractive index n mounted at a 45° angle to the direction of incoming light are given respectively by(9)

$$R = -r\frac{1-e^{i\phi}}{1-r^2e^{i\phi}} \quad \text{and} \quad T = (1-r^2)\frac{e^{i\phi/2}}{1-r^2e^{i\phi}}, \quad (9)$$

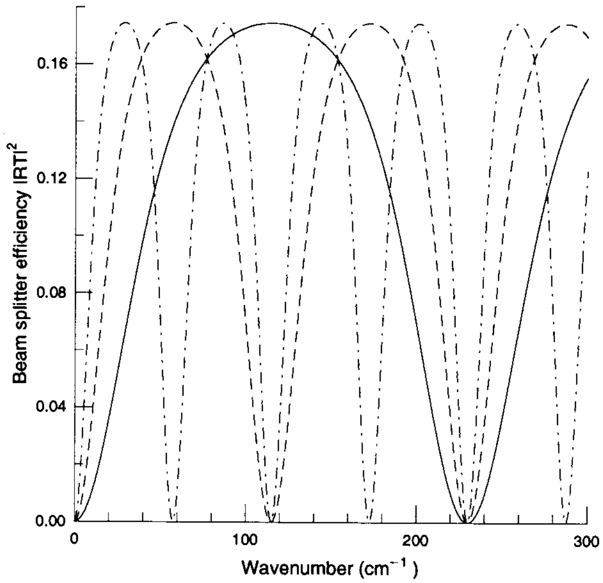

FIGURE 2. The efficiency of Mylar beam splitter as a function of frequency for different thicknesses: 12.7 (solid), 25.4 (dashed), and 50.8 μm (dash-dotted line).

where r is the amplitude reflection coefficient of the air-to-Mylar interface at an incident angle of 45°, and ϕ defined as $4\pi t\sigma\sqrt{(2n^2-1)/2}$ at wavenumber $\sigma = 1/\lambda(10)$. No absorption in the foil is assumed, and the refractive index is assumed to be constant ($n = 1.85$) over all frequencies(10).

The efficiency of the beam splitter defined as $|RT|^2$ is shown in Fig. 2. The efficiency becomes zero at frequencies where light reflected from both surfaces of the beam splitter interferes destructively. Equations in the time domain such as Eq. (4) are no longer valid for the case of varying efficiency and need to be replaced by appropriate convolution integrals; however, equations in the frequency domain such as Eq. (5) still hold. The width of the interferogram can not be directly used for bunch-length estimation unless interference effects on the interferogram are included.

Bunch-Length Analysis

The interference effects are studied numerically for both Gaussian and rectangular bunch distributions, and the bunch length is then estimated from this study. Although most real bunch distributions are neither Gaussian nor rectangular, the bunch lengths estimated from the two distributions will give reasonable bounds for the real one.

Examples of the beam-splitter interference effects on a rectangular bunch distribution are shown in Fig. 3. For an ideal beam splitter, the interferogram is non-negative and has the expected triangular peak with its FWHM equal to the bunch length [c.f., Fig. 3(a)]. For Mylar beam splitters, negative valleys

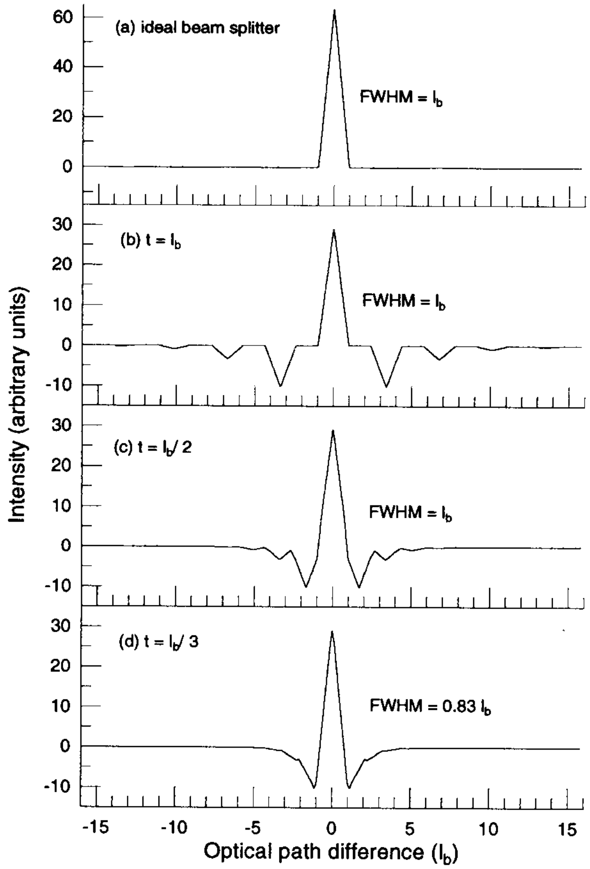

FIGURE 3. The simulation of the beam-splitter interference effects on a rectangular bunch distribution with different beam splitters: (a) an ideal beam splitter and Mylar beam splitters of thicknesses (t) (b) equal to, (c) half, and (d) one third of the bunch length (l_b).

appear in the interferograms, which are due to suppression of the low frequency area by the first zero of the beam-splitter efficiency. These valleys move closer to the main peak as the beam-splitter thickness (t) decreases [c.f., Fig. 3(b)–(d)]. For beam splitters thinner than about half the bunch length (l_b), they merge with the main peak and make the peak narrower [c.f., Fig. 3(d)]. The effects are similar for a Gaussian distribution. Detailed results on how the FWHM values in the interferogram change with the equivalent bunch length for both Gaussian and rectangular distributions are shown in Fig. 4. Once the beam splitter is chosen, the bunch length can be derived from the measured interferogram width with the help of Fig. 4.

EXPERIMENTAL SETUP

For this experiment, the SUNSHINE facility was operated to produce 1-μs-long electron macro-pulses at 10 Hz containing a train of about 3000 electron bunches at an energy of 30 MeV. Each bunch had about 3.5×10^7 electrons.

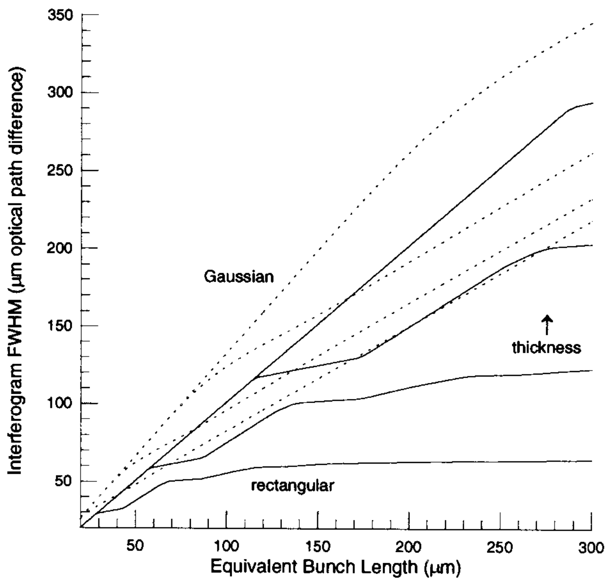

FIGURE 4. Interferogram FWHM's as functions of equivalent bunch lengths of both Gaussian (dotted lines) and rectangular (solid lines) bunch distributions for different Mylar beam-splitter thicknesses: 12.7, 25.4, 50.8, and 127 μm. Within the same distribution, the lines are shown from the bottom to the top in the increasing order of thickness.

As shown in Fig. 1, transition radiation is generated when the electrons pass through an Al foil. The divergent backward transition radiation is extracted from the evacuated beam line into air via a high-density polyethylene (HDPE) window and is converted into parallel light by an off-axis paraboloidal mirror. The parallel light then enters a far-infrared Michelson interferometer.

The interferometer consists of a Mylar beam splitter mounted at a 45° angle to the direction of incident light, a fixed and a movable first-surface mirror, and a room-temperature detector. The movable mirror is moved by a linear actuator via a PC. The detector consists of a Molectron P1-65 $LiTaO_3$ pyroelectric bolometer of 5 mm diameter and a pre-amplifier. The detector signal is digitized into the computer. With the computer interfaces, the autocorrelation measurements are performed automatically through the program under the LabVIEW control environment implemented on the computer.

RESULTS AND DISCUSSION

By measuring the detector signal as a function of the position of the movable mirror via the computer program, the interferograms of 2.2 mm long with 5-μm mirror step size are measured for four different Mylar beam-splitter thicknesses and shown in Fig. 5. This 5-μm mirror step size corresponding to a 33-fs time resolution is good enough for the experiments; however, a subfemtosecond resolution can still be achieved by the actuator with a submicron step size.

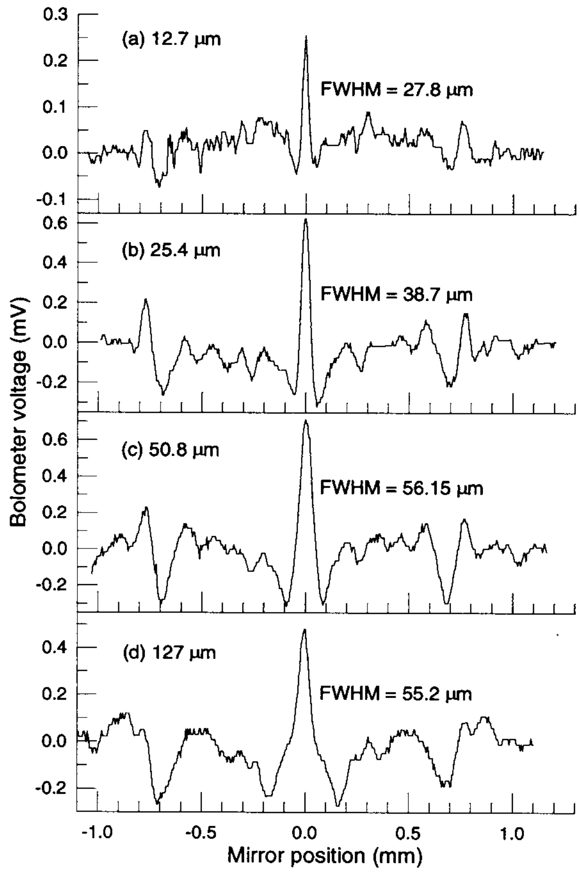

FIGURE 5. Interferograms measured for different Mylar beam-splitter thicknesses: (a) 12.7, (b) 25.4, (c) 50.8, and (d) 127 μm. The FWHM's of the main peaks are measured in mirror movement, which are half of widths in optical path difference.

The beam parameters are kept the same when different beam splitters are used. The valleys around the main peak are separated farther apart as the beam-splitter thickness increases. This widens the main peak [c.f., Fig. 5(a)–(c)] until the valleys are out of the peak [c.f., Fig. 5(c),(d)]. The base of the peak can even be seen in Fig. 5(d). The measured interferogram FWHM's and the estimated equivalent bunch lengths deduced from Fig. 4 for Gaussian and rectangular distributions are shown in Table 1. The estimated bunch lengths provide intervals for the real bunch length and are consistent over a 10-fold change in the beam-splitter thickness. The estimated real bunch length is about 100 μm (0.33 ps) long.

CONCLUSION

In conclusion, a new frequency-resolved bunch-length measuring method specialized for subpicosecond electron pulses has been developed at the Stanford SUNSHINE facility. This method measures the autocorrelation of co-

TABLE 1. Measured interferogram FWHM's in optical path difference (OPD) for different beam-splitter thicknesses and the corresponding estimated equivalent bunch lengths deduced from Fig. 4 for Gaussian and rectangular distributions.

Beam splitter thickness (μm)	Interferogram FWHM OPD (μm)	Estimated equivalent bunch length (μm) Gaussian	Rectangular
12.7	55.6	60.8	100.6
25.4	77.4	72.8	103.2
50.8	112.3	86.9	111.0
127.0	110.4	83.1	109.1

herent transition radiation emitted from electron bunches via a far-infrared Michelson interferometer. Measurements have verified this method by showing consistent results over a broad range of beam-splitter thicknesses. This autocorrelation method demonstrates good subpicosecond resolving power beyond the reach of existing time-resolved methods. This work is supported by the Department of Energy (Contract No. DE-AC03-76F00515).

REFERENCES

1. R. L. Fork, B. I. Greene, and C. V. Shank, Appl. Phys. Lett. **38**, 671 (1981).
2. W. Barry, in *Proceedings of the Workshop on Advanced Beam Instrumentation* **1**, KEK, Tsukuba, Japan, April 22-24, 1991 (unpublished); CEBAF Preprint No. PR-91-012.
3. P. Kung, H.-C. Lihn, D. Bocek, and H. Wiedemann, Proc. SPIE **2118**, 191 (1994).
4. P. Kung, H.-C. Lihn, D. Bocek, and H. Wiedemann, Phys. Rev. Lett. **73**, 967 (1994).
5. H.-C. Lihn, P. Kung, C. Settakorn, D. Bocek, and H. Wiedemann, Phys. Rev. E, submitted; SLAC PUB-95-6958.
6. V. L. Ginsburg and I. M. Frank, Zh. Eksp. Teor. Fiz. **16**, 15 (1946).
7. J. S. Nodvic and D. S. Saxon, Phys. Rev. **96**, 180 (1954).
8. E. Hecht and A. Zajac, *Optics* (Addison-Wesley, Reading, Massachusetts, 1974), Sec. 9.7.
9. G. W. Chantry, *Submillimetre Spectroscopy* (Academic Press, London, 1971), App. A.
10. R. J. Bell, *Introductory Fourier Transform Spectroscopy* (Academic Press, London, 1972), Ch. 9.